electronics

MDPI

Article

Extending Field Deployment of Wireless Personal Use Monitors via STM32L4 Low-Power Configurations

Joshua D. Butler [1], Edward C. Hensel [2,*], Noah Meltzer [3] and Risa J. Robinson [2]

[1] Department of Information and Computing Studies, Rochester Institute of Technology, Rochester, NY 14623, USA
[2] Department of Mechanical Engineering, Rochester Institute of Technology, Rochester, NY 14623, USA
[3] Department of Electrical Engineering, Rochester Institute of Technology, Rochester, NY 14623, USA
* Correspondence: echeme@rit.edu

Abstract

Limited battery life in previous generations of the wireless Personal Use Monitor (wPUM) required frequent recharging during ambulatory studies and increased the risk of missing puff-topography data. The fourth-generation wPUM was designed around an STM32L433 microcontroller using low-power operating modes and an event-driven architecture. Pressure-sensor interrupts wake the microcontroller during puff activity, while periodic alarms initiate device-health monitoring. This study evaluated four STM32L4 low-power configurations—Sleep, STOP0, STOP1, and STOP2—using twenty devices, with five assigned to each mode under a standardized sensing and logging workload. Mean standby runtime was 3.27 days for Sleep, 27.78 days for STOP0, 30.15 days for STOP1, and 31.38 days for STOP2. STOP2 achieved the longest mean standby runtime with the lowest observed reliability among the STOP modes, this result was based on only two valid datasets. STOP1 had consistent operations across four valid datasets, making it the preferred configuration for extended ambulatory deployment. These findings demonstrate that low-power mode selection for embedded sensing systems must consider wake reliability in addition to power consumption.

Keywords: low-power electronics; microcontroller; wearable sensors; battery life

1. Introduction

In the last two decades, our research lab has investigated how relationships between tobacco product characteristics and product use behavior may influence a user's exposure to hazardous and potentially hazardous compounds. Use behavior is traditionally quantified for each study participant's puff topography (time of day, puff flow rate, and duration) in their natural environment [1–4]. Previous evaluations of portable puff-topography monitors have identified limitations in measurement accuracy, puff detection, and data recording, highlighting the importance of collecting data during deployment in natural environments [5,6].

The Respiratory Technologies Lab (RTL) at Rochester Institute of Technology develops custom technology to enable aerosol science investigation, with a particular focus on ambulatory observation of inhaled aerosols. Technologies developed at RTL support respiratory assessment and protection, in vitro toxicology and aerosol emissions characterization, computational modeling, and data fusion tools. Of particular interest to this manuscript, the lab has deployed wearable respiration monitors (WRM™) to record lung inhalation behavior topography and developed wireless Personal Use Monitors (wPUM™) to record how human subjects interact with tobacco products via puffing behavior, while mimicking a form

Check for updates

Academic Editor: Jichai Jeong

Received: 28 September 2026
Revised: 24 October 2026
Accepted: 26 October 2026
Published: 28 October 2026

Copyright: © 2026 by the authors. Licensee MDPI, Basel, Switzerland. This article is an open access article distributed under the terms and conditions of the Creative Commons Attribution (CC BY) license.

factor similar to their preferred electronic nicotine delivery system (ENDS), combustible cigarettes, or hookah [7].

To date, three generations of wPUM puff topography monitors have been deployed in eight natural-environment observational studies (OSs) annotated as OS1–OS8. These identifiers refer to individual studies conducted by the research laboratory to characterize tobacco product use under natural conditions. Each study involved different tobacco products, participant populations, or observation periods. The Gen 1 wPUM monitor was introduced in 2013 and deployed to 22 OS1 participants for a 24 h period and used to monitor puffing behavior in users vaping a first-generation cig-a-like disposable ENDS. The Gen 1 monitor used an Atmel Atmega 328P microcontroller on a TinyLily board, with a MicroSD card for storage and two primary lithium battery cells for power. The Gen 2 wPUM monitor was introduced in 2015 and has been deployed to 20 participants for one week using Pen-Style ENDS (OS2), 34 participants using NJoy Pen-Style ENDS (Manufactured by NJOY LLC, Purchased from a Retail Vendor in Rochester, NY USA) in a two-week flavor-switching study (OS3), 34 participants for a one-week hookah study (OS4 Phase 1), and 26 participants for a one-week cigarette study (OS4 Phase 2) [8]. The Gen 2 monitor also used an Atmega32P MCU on a custom board, with a Micro SD card for storage and two primary cells for power. The Gen 3 monitor was introduced in 2019 and has been deployed to 16 participants for a one-week study of dual use of hookah and cigarettes (OS4 Phase 3), 10 participants using a variety of ENDS devices in a limited deployment (OS5 and OS6), 45 participants in a two-week switching study on nicotine concentration (OS7), and 38 participants to date in a one-week observation period of a variety of ENDS products (OS8, currently in progress). The Gen 3 monitor used an STM32F401R MCU on a proprietary board with on-board flash memory and 150/350 mAh rechargeable LiPO cells [9]. The Gen 4 wPUM, introduced here, is planned for use in human subject studies during late 2026.

Limited battery life was a common theme of earlier generations of the wPUM monitors. Battery performance and energy management are also important design considerations in healthcare and biomedical devices, where reliable operation is needed over extended periods [10,11]. Previous generation monitors provided one-day runtime and required participants to recharge the monitors frequently during the observational deployment. Failure to recharge the monitor, or failure to recognize that the battery is depleted, could result in loss of puff-topography data and reduce the usefulness of a deployment. The limited deployment runtime of the third-generation wPUM was primarily associated with its architecture design. Because the pressure sensor does not provide a suitable interrupt mechanism to detect puff activities, the microcontroller remains active by continuously polling the sensor and recording puff-topography data, resulting in increased current consumption during long periods in which no puff occurred.

Previous generation wPUM deployments have involved observation periods ranging from 24 h to two weeks. For the fourth-generation monitor, the design objective is to gain sufficient battery life to support an entire deployment period without requiring participants to recharge the device. A minimum deployment duration of 14 days would accommodate the longest completed observation periods described in this study. Extending battery life beyond this duration would provide additional operational flexibility and reduce the risk of data loss associated with battery depletion.

Independent studies have investigated the effects of system design, task scheduling, and processor power management on energy consumption and battery runtime in embedded systems [12–14]. Building on these principles, the fourth-generation wPUM monitor was developed to address battery-life limitations of previous generations by incorporating a low-power microcontroller (MCU) such as the STMicroelectronics STM32L4 series (Geneva,

Switzerland) and an event-driven architecture. Unlike the previous polling-based design, the new system utilizes pressure-sensor interrupts to initiate puff-topography recording while the MCU remains in a low-power state during periods of inactivity. This approach is intended to extend battery life, reduce participant charging burden, and minimize the risk of missing puff-topography data during natural environment deployment.

Previous research demonstrated the importance of estimating battery lifetime in wireless sensing systems and evaluating battery performance under real-world deployment conditions [15,16]. Battery-state monitoring has also been investigated using STM32-based embedded systems [17]. This paper evaluates several microcontroller low-power configurations of the fourth-generation wPUM monitor under controlled conditions to identify the preferred low-power configuration for extending standby runtime. While the fourth-generation wPUM is an event-driven monitor, this is the intended architecture, not the workload tested in this paper. The configurations are compared based on standby runtime and reliability to identify which low-power configuration is suitable for extended deployment with the study participants. The results demonstrate the trade-offs between battery consumption, reliable behavior, and continuous event-driven monitoring in a battery-powered embedded system.

2. Materials and Methods

2.1. Fourth-Generation wPUM System Architecture

The fourth-generation wPUM device is a battery-powered device that uses an event-driven architecture to wake from low-power mode to capture puff-topography data during natural-environment tobacco product use. The system uses an STM32L4 series microcontroller (MCU), STMicroelectronics LPS27HHW pressure sensors [18], external flash memory, fuel-gauge circuitry, a battery management system, and a rechargeable lithium-polymer battery. Figure 1 illustrates the general hardware components and the event-driven monitoring architecture.

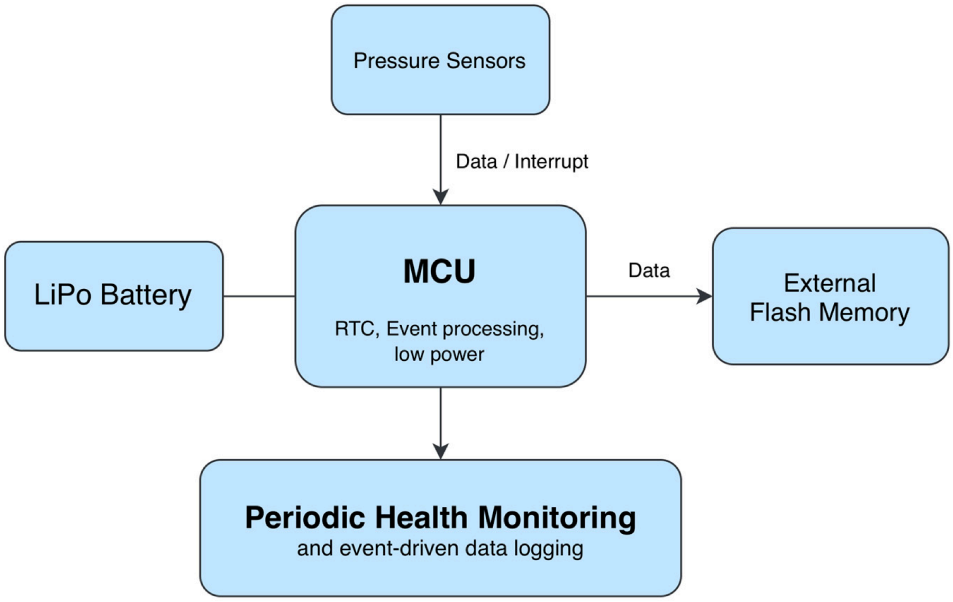


Figure 1. Fourth-generation wPUM system architecture.

Unlike previous generations, which used a polling-based architecture to continuously monitor pressure changes, the fourth-generation device uses pressure sensor interrupts

to wake the MCU from its low-power mode. The pressure sensors continuously monitor pressure changes and generate an interrupt when a predefined threshold is reached.

In addition to puff event activities, the MCU's real-time clock (RTC) alarm is used to schedule periodic device-health monitoring. The RTC generates an alarm every 60 s to wake the system and record pressure, temperature, and battery health data independently of puffing activity. This periodic monitoring allows the system to record device-health information even when no puff activity occurs.

The purpose of this study is to evaluate the standby runtime of the fourth-generation wPUM under different MCU low-power configurations. The experiment simulated standby behavior without puff events while maintaining periodic device-health monitoring every 60 s. Each device continued operating under the assigned low-power configuration until battery depletion or premature termination. This approach allowed the configurations to be compared under a standardized workload.

2.2. Experimental Design and Test Setup

The STM32L4 series provides several low-power operating modes with different power consumption and wake-up characteristics [19]. Twenty (20) fourth-generation wPUM devices were evaluated under four microcontroller low-power configurations: Sleep, STOP0, STOP1, and STOP2. Five (5) devices were assigned to each low-power configuration. Each device was powered by a 350 mAh lithium-polymer battery. Each battery was charged before testing, with full-charge status verified during dataset review.

A total of 8 of the 20 batteries were acquired a little over six months before the experiment. To minimize potential differences in battery performance associated with battery age, they were randomly distributed across the four low-power configurations. Table 1 summarizes the battery assignments and calculated battery ages (in days) at the beginning of testing. The battery age is the elapsed time in days since purchase lot date, not necessarily the actual manufacturing age. State-of-charge (SOC) values were obtained from the Maxim Integrated's MAX17048 fuel-gauge IC using its Li+ battery-modeling algorithm ModelGauge™ [20]. Values exceeding 100% represent unadjusted fuel-gauge estimates and do not indicate battery capacity exceeding its rated maximum. Although battery age was recognized as a potential source of runtime variation, it was not treated as a primary experimental factor.

Table 1. Battery identification, age, and distribution across STM32L4 low-power configurations at the start of testing. Footnote a: * = Not fully charged; † = bad data; ‡ = premature termination.

Mode	MCU Serial [a]	Battery ID	Purchase Lot Date	Start Date	Initial SOC	Initial Voltage (V)	Battery Age (Days)
Sleep	0022005546	215	2025-06-12	2025-06-26	109%	4.26	14
Sleep	0028005446	203	2025-01-13	2025-06-28	101%	4.31	166
Sleep	003A004D46	204	2025-01-13	2025-06-29	108%	4.25	167
Sleep	004B005546	214	2025-06-12	2025-06-29	107%	4.24	17
Sleep	006B005646	218	2025-06-12	2025-07-08	110%	4.28	26
STOP0	0020005346	222	2025-06-12	2025-06-30	110%	4.27	18
STOP0	0044004C46	207	2025-01-13	2025-06-27	116%	3.95	165
STOP0	0050004C46 *	219	2025-06-12	2025-06-25	67%	3.92	13
STOP0	005E005746	208	2025-01-13	2025-06-27	111%	4.28	165
STOP0	0069005446	223	2025-06-12	2025-06-25	126%	4.23	13
STOP1	0025005846	213	2025-06-12	2025-06-27	107%	4.30	15
STOP1	0031004D46	202	2025-01-13	2025-06-27	102%	4.30	165
STOP1	0041005346	220	2025-06-12	2025-06-30	110%	4.26	18

Table 1. *Cont.*

Mode	MCU Serial [a]	Battery ID	Purchase Lot Date	Start Date	Initial SOC	Initial Voltage (V)	Battery Age (Days)
STOP1	0047005346	206	2025-01-13	2025-06-27	111%	4.28	165
STOP1	005D005546 *	224	2025-06-12	2025-06-27	38%	3.80	15
STOP2	0034005846	209	2025-01-13	2025-06-27	101%	4.29	165
STOP2	003E004D46 ‡	205	2025-01-13	2025-06-30	110%	4.26	168
STOP2	0040004D46	221	2025-06-12	2025-06-27	110%	4.30	15
STOP2	0053005C46 †	216	2025-06-12	2025-06-25	0%	5.07	13
STOP2	0063005346 *,‡	217	2025-06-12	2025-06-25	78%	3.94	13

The experiment was designed for autonomous operation. Due to low current consumption in the MCU's low-power mode, the experiment is expected to run over an extended period. Devices under test (DUTs) were programmed and configured to operate continuously without any manual intervention until the battery is fully depleted and the MCU experiences a brownout and ceases to run.

The pressure sensors (LPS27HHW) were mounted on the underside of the fourth-generation wPUM board. To prevent obstruction of the sensors and to permit exposure to ambient environmental conditions, each device was placed on cut-out cardboard to support the fixture while exposing the sensors to the environment. Batteries were positioned away from the board to help prevent the board from falling off the fixture. Testing was conducted under ambient office conditions in an air-conditioned setting.

2.3. Firmware Workload and Low-Power Configurations

Test firmware was developed in C using STM32CubeIDE [21] and programmed onto the STM32L433-series microcontroller of each DUT. The experiment groups used identical firmware configurations except for the low-power mode selected during inactive periods.

Table 2 summarizes the characteristics of the evaluated operating modes and their estimated current consumption. The STM32CubeMX [22] power-consumption estimation utility was used to obtain the current consumption values under the configured MCU operating conditions. The Gen 4 wPUM will operate at 1.8 V, running at 48 MHz. These model-based estimates represent MCU current consumption and do not account for all external components of the wPUM system, including the pressure sensors and external flash memory. Therefore, the values provide a relative comparison of the operating modes rather than measurements of total device current consumption.

Table 2. Characteristics and estimated current consumption of STM32L4 series operating modes.

Mode	MCU State	Clock Operation	Peripheral Availability	Estimated MCU Current Consumption
Run	Active	MCU operates at 48 MHz @ 1.8 V	All peripherals operate normally	5.04 mA
Sleep	Stopped	Peripheral clocks remain active	Most peripherals and DMA continue operating	2.21 mA
STOP0	Stopped	High-speed clocks disabled	Broad low-power peripheral and wake-up support	108 µA

Table 2. *Cont.*

Mode	MCU State	Clock Operation	Peripheral Availability	Estimated MCU Current Consumption
STOP1	Stopped	High-speed clocks disabled	Similar to Stop 0, with slightly longer wake-up time	4.34 µA
STOP2	Stopped	Most internal clocks and power domains disabled	Limited to RTC, LPTIM1, I^2C3, LPUART, and selected monitoring peripherals	995 nA

During each test cycle, each device performed the following sequence:

1. The MCU exited the assigned low-power mode.
2. The device acquired pressure and temperature data from each pressure sensor.
3. The device acquired battery state data.
4. The light-emitting diode (LED) indicator was activated for one second.
5. The resulting timestamp, sensor readings, and battery health data were written to the onboard external flash memory.
6. The MCU returned to its assigned low-power mode.

The sequence was repeated every 60 s for the duration of the battery life. The firmware's periodic workload simulated the health-check operation during field deployment, in which the wPUM monitor remains in a low-power state between puff events but wakes occasionally to record health data. The MCU wakes at a 60 s interval by a built-in MCU real-time clock (RTC) alarm to read sensor data, perform LED indications, and handle flash-memory operations, allowing a standardized workload for comparing the four low-power configurations.

All devices used the same sensor configuration, sampling sequence, LED behavior, flash-memory operations, and wake interval. The firmware continued operating until the battery was depleted and the MCU failed to wake from low-power mode due to power loss.

2.4. Data Recording and Outcome Measures

Data recorded in the external flash memory were retrieved through the serial interface following completion of each experimental trial. Each device recorded timestamps, pressure readings, temperature readings, and battery state information during every monitoring cycle.

The primary outcome was standby runtime, defined as the elapsed time between disconnection after fully charging the battery and the final recorded data during a wake cycle. Secondary outcomes included the number of completed wake cycles, recorded battery voltage, SOC, pressure readings, temperature readings, any instance of incomplete or corrupted data, and reliability of low-power operation to perform the tasks consistently over the entire battery life duration.

Operational reliability was assessed by examining the continuity of timestamped records and identifying unexpected interruptions in data acquisition. Trials that terminated before confirmed battery depletion were identified separately to distinguish premature operational failures from battery-limited runtime.

2.5. Statistical Analysis

For each low-power configuration, standby runtime was analyzed and reported using the minimum, mean, and maximum values. Each dataset was examined for valid timestamps, battery SOC measurements, potential experimental anomalies, and the continuity

of data recording throughout the entire experimental period. Trials that did not meet the data-quality criteria were excluded from standby runtime analysis.

Standby runtime statistics were calculated using datasets that met the inclusion criteria, while excluded datasets were retained for the assessment of operational reliability. Therefore, the reported mean runtime represents the performance of valid trials rather than the overall performance of all devices assigned to each low-power configuration.

3. Results

Before performing the data analysis, all datasets were reviewed for completeness, data integrity, and consistency with the experiment protocol. The review uncovered several issues, including premature termination of data recording, an incompletely charged battery, and a fuel-gauge malfunction. Table 3 summarizes the exclusion reasons for some devices. The remaining datasets were used to determine the standby runtime and compare all low-power configurations.

Table 3. Excluded devices and reasons for exclusion from the standby runtime analysis.

Mode	MCU Serial	Reason for Exclusion
STOP0	0050004C46	Battery was not fully charged
STOP1	005D005546	Battery was not fully charged
STOP2	003E004D46	Premature termination/unknown reason
STOP2	0053005C46	Fuel gauge failure
STOP2	0063005346	Premature termination/unknown reason

Figure 2 shows the battery SOC curves for all devices with valid datasets grouped by low-power configuration. Sleep devices discharged faster and stopped operating after three days. STOP0 device runtimes range from 23 to 31 days, but their discharge profiles varied among devices. STOP1 devices showed consistent discharge curves and ranged from 28 to 31 days. The two valid STOP2 devices ranged from 31 to 32 days and showed discharge profiles similar to STOP0 and STOP1. The remaining STOP2 devices were excluded from analysis because of premature termination or invalid battery-health data.

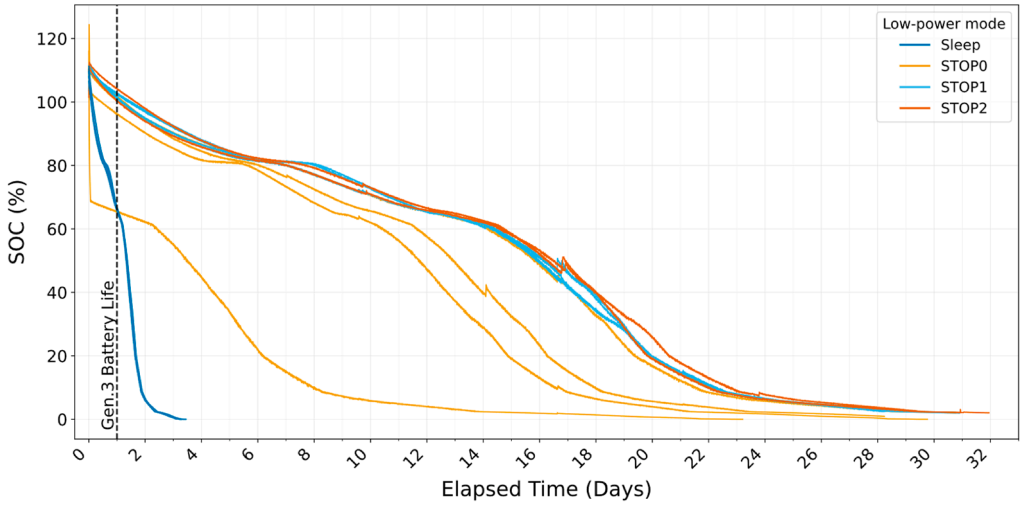


Figure 2. Battery SOC curves for fourth-generation wPUM devices operating in each mode. Only datasets meeting the inclusion criteria are shown: Sleep ($n = 5$), STOP0 ($n = 4$), STOP1 ($n = 4$), and STOP2 ($n = 2$). Each curve represents one device.

The low-power configurations substantially extended device operation relative to Sleep mode. Figure 3 presents the mean standby runtime with a scatter plot of individual devices. Although STOP2 achieved the longest mean standby runtime, it exhibited low reliability with only two valid datasets. The limited sample size and operational anomalies observed in three devices raise concerns about the reliability of STOP2 low-power mode. In contrast, STOP1 achieved a slightly shorter standby runtime than STOP2 but operated consistently across its valid trials, providing a more dependable balance between extended standby runtime and reliability.

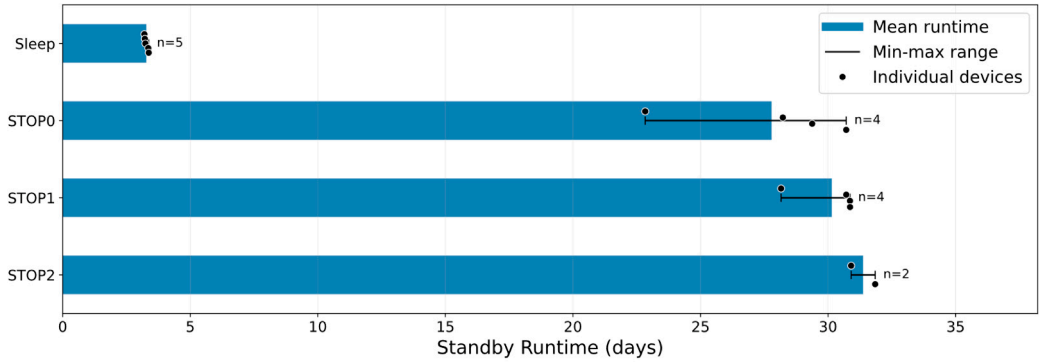


Figure 3. Mean standby runtime of fourth-generation wPUM devices by low-power configuration. Error bars indicate the minimum and maximum observed standby runtime, and individual data points represent the standby runtime of each device. Only valid datasets were included.

4. Discussion

This study assessed the operational outcomes of four low-power configurations of the STM32L433 microcontroller in the fourth-generation wPUM monitor. The key finding was that STOP1 provided the best balance of standby runtime and reliable wake behavior, achieving an average runtime of 30.15 days. Although STOP2 achieved the longest mean standby runtime of 31.38 days among valid trials, this result was based on only two datasets. Two of the five devices failed to resume normal operations following RTC wake events, and one failed to record battery state-of-charge values. This highlights the importance of evaluating low-power configurations based not only on current consumption but also on wake-up reliability, clock configuration, timestamp integrity, and successful resumption of sensing and data logging operations. Sleep mode produced a mean standby runtime of 3.27 days, showing a modest improvement over the one-day runtime of the third-generation wPUM board. This improvement can be attributed to differences in firmware architecture. While fourth-generation firmware reduced MCU activity during low-power periods, the third-generation firmware runs in continuous polling mode to check for active puff activity. Despite the increased runtime, sleep mode does not meaningfully reduce participant charging burden or lower the risk of missed data due to battery depletion.

Both STOP0 and STOP1 substantially extended standby runtime compared with Sleep mode. STOP0 achieved a mean runtime of 27.78 days ($n = 4$), whereas STOP1 achieved 30.15 days ($n = 4$), and STOP2 achieved 31.38 days ($n = 2$). STOP0 and STOP1 showed high reliability while STOP2 exhibited wake-up issues. These findings suggest that STOP1 provided the optimal balance between extended standby runtime and dependable system operation for ambulatory deployment.

The STMicroelectronics application note (AN4621) states that STOP2 preserves SRAM contents and execution context, although the system clock may need to be configured after wake-up [23]. In addition, the STM32L433 device errata document (ES0318) identifies several operating conditions that may affect transitions into and out of STOP modes, including

clock-related behavior and brown-out reset conditions [24]. These factors may contribute to the observed anomalies but were not independently verified in this experiment. The failure to resume normal operations in two STOP2 devices suggests an unresolved firmware or hardware dependent issue. The exact cause could not be established, and further diagnostic testing is needed to determine whether the failures happened during wake-up or during subsequent firmware execution. Therefore, the observed failures should not be interpreted as an inherent limitation of STOP2 mode itself but rather as a reliability concern associated with the fourth-generation wPUM implementation tested in this study.

Further investigation is warranted to identify the source of these anomalies and evaluate the practicality of STOP2 mode for future wPUM implementations. Although STOP2 achieved a longer mean standby runtime, the findings do not provide sufficient evidence to establish reliable operation across all tested devices. Until these issues are resolved, STOP1 represents the more dependable configuration for the fourth-generation wPUM.

The standby runtime observed in this study should be interpreted in the context of the intended application. Previous wPUM observational studies have required monitoring periods of up to two weeks. The minimum standby runtime of 28.18 days achieved with STOP1 substantially exceeds this historical observation period under the standardized experimental workload, suggesting that the fourth-generation architecture may reduce or eliminate the need for intermediate charging.

However, the experimental workload described above does not reproduce actual puff-triggered activities during natural-environment monitoring. The actual operational runtime will depend on the frequency and duration of puff events by participants, sensor sampling activity, and data storage-related operations. This experiment is exploratory and aims to determine if it is feasible to achieve a longer standby time during natural-environment deployment. Therefore, the standby runtime measurements should be considered baseline performance under limited, controlled conditions rather than a direct prediction of operational runtime during deployment. Additional validation testing is needed under a simulated laboratory puff-topography environment to establish operational deployment runtime.

A larger-capacity battery could further extend operational runtime. However, increasing battery capacity may also increase the wPUM monitor's size and weight, which is designed to resemble the tobacco products used by study participants. These constraints must be considered when evaluating battery alternatives. This study did not evaluate the feasibility of using a larger-capacity battery, as the primary goal was to assess the standby runtime of the fourth-generation wPUM devices using the existing battery used in previous generations.

This study has several limitations. First, the sample size was limited to five devices per low-power configuration, with some datasets being excluded because they did not meet the data-quality criteria. In particular, only two valid datasets were available for STOP2, limiting the confidence in its estimated mean runtime. Second, testing was performed in a stable, controlled environment with a repetitive workload that did not fully reproduce natural ENDS use, such as variable puff topography, changing environmental conditions, and typical participant behavior. Battery age and prior usage history were also not identical across all devices and may have contributed to standby runtime variability. In addition, two STOP2 trials ended early because of unresolved operational failures following RTC alarm wake-up events rather than confirmed battery depletion. Finally, the findings are specific to the fourth-generation wPUM hardware and firmware configuration, and future work should be validated under simulated puff-topography conditions and during ambulatory human-subject deployment.

5. Conclusions

This study showed that selecting the correct low-power configuration for an embedded system requires consideration of both current consumption and operational reliability. Although STOP2 achieved the longest mean standby runtime, the result was based on only two valid datasets, with unresolved operational anomalies in two devices and invalid battery-health recording in one device. STOP1 exhibited significant improvement over the one-day runtime of the third-generation device with consistently high reliability. Based on the experimental findings, STOP1 was the preferred low-power mode for extended ambulatory deployment of the fourth-generation wPUM monitor. This finding suggests that the fourth-generation wPUM has the potential to support extended ambulatory deployment with reduced participants' burden to charge the device daily. Further validation under actual puff-monitoring conditions is needed to establish operational runtime during field deployment.

Author Contributions: Conceptualization, J.D.B. and E.C.H.; methodology, J.D.B., E.C.H., and N.M.; software, J.D.B.; validation, E.C.H.; formal analysis, J.D.B. and E.C.H.; investigation, J.D.B. and N.M.; resources, E.C.H. and R.J.R.; data curation, J.D.B. and N.M.; writing—original draft preparation, J.D.B. and E.C.H.; writing—review and editing, R.J.R.; visualization, J.D.B. and N.M.; supervision, E.C.H. and R.J.R.; project administration, E.C.H.; funding acquisition, E.C.H. and R.J.R. All authors have read and agreed to the published version of the manuscript.

Funding: This work was supported in part by the National Institute on Drug Abuse of the National Institutes of Health under Award Number R01DA057687. The content is solely the responsibility of the authors and does not necessarily represent the official views of the National Institutes of Health.

Data Availability Statement: Dataset available on request from the authors.

Acknowledgments: During the preparation of this manuscript, the author(s) used OpenAI ChatGPT (GPT-4o) and Grammarly for the purposes of language editing, organization, and refinement of selected portions of this manuscript. The tool was used to improve clarity, conciseness, grammar, and overall presentation of text drafted by the authors. All technical content, experimental design, data analysis, interpretation of results, and conclusions were developed and verified by the authors. The authors reviewed and revised all AI-assisted text and take full responsibility for the content of this publication.

Conflicts of Interest: The authors declare no conflicts of interest.

Abbreviations

The following abbreviations are used in this manuscript:

DMA	Direct memory access
DUT	Device under test
ENDS	Electronic nicotine delivery system
I^2C	Inter-integrated circuit
IC	Integrated circuit
LED	Light-emitting diode
LiPo	Lithium-polymer
LPTIM	Low-power timer
LPUART	Low-power universal asynchronous receiver/transmitter
MCU	Microcontroller
OS	Observational study
RTC	Real-time clock
RTL	Respiratory Technologies Lab
SOC	State of charge
SRAM	Static random-access memory
wPUM	Wireless personal use monitor
WRM	Wearable respiration monitor

References

1. Hammond, D.; Fong, G.T.; Cummings, K.M.; Hyland, A. Smoking Topography, Brand Switching, and Nicotine Delivery: Results from an in Vivo Study. *Cancer Epidemiol. Biomark. Prev.* **2005**, *14*, 1370–1375. [CrossRef] [PubMed]
2. Spindle, T.R.; Breland, A.B.; Karaoghlanian, N.V.; Shihadeh, A.L.; Eissenberg, T. Preliminary Results of an Examination of Electronic Cigarette User Puff Topography: The Effect of a Mouthpiece-Based Topography Measurement Device on Plasma Nicotine and Subjective Effects. *Nicotine Tob. Res.* **2015**, *17*, 142–149. [CrossRef] [PubMed]
3. Bridges, R.B.; Combs, J.G.; Humble, J.W.; Turbek, J.A.; Rehm, S.R.; Haley, N.J. Puffing Topography as a Determinant of Smoke Exposure. *Pharmacol. Biochem. Behav.* **1990**, *37*, 29–39. [CrossRef] [PubMed]
4. Ossip-Klein, D.J.; Martin, J.E.; Lomax, B.D.; Prue, D.M.; Davis, C.J. Assessment of Smoking Topography Generalization across Laboratory, Clinical, and Naturalistic Settings. *Addict Behav.* **1983**, *8*, 11–17. [CrossRef] [PubMed]
5. Mikheev, V.B.; Buehler, S.S.; Brinkman, M.C.; Granville, C.A.; Lane, T.E.; Ivanov, A.; Cross, K.M.; Clark, P.I. The Application of Commercially Available Mobile Cigarette Topography Devices for E-Cigarette Vaping Behavior Measurements. *Nicotine Tob. Res.* **2020**, *22*, 681–688. [CrossRef] [PubMed]
6. Oldham, M.J.; Plunkett, S.E.; Fisher, M.T.; Shafer, K.H.; Morton, M.J. Laboratory Evaluation of the CReSSmicro™ Portable Topography Device: Implications for Clinical Research. *Contrib. Tob. Res.* **2014**, *26*, 19–25. [CrossRef]
7. Robinson, R.; Sarles, S.; Meyers, B.; Eddingsaas, N.; Hensel, E. Design of the wPUM™ Family of Topography Monitors for Natural Environment Observation of Tobacco Product Use. In Proceedings of the 2018 Tobacco Regulatory Science Meeting, Bethesda, MD, USA, 18–20 June 2018.
8. Robinson, R.J.; Jayasekera, S.; DiFrancesco, G.; Hensel, E.C. Characterization and Validation of the Second-Generation wPUM Topography Monitors. *Nicotine Tob. Res.* **2021**, *23*, 390–396. [CrossRef] [PubMed]
9. Meyers, B.T.; Hensel, E.C.; Jayasekera, S.; Robinson, R.J. Characterization of the wPUM™ Generation 3 Topography Monitors. In Proceedings of the 2019 BMES Annual Meeting Biomedical Engineering Society (BMES), Philadelphia, PA, USA, 16–19 October 2019.
10. Nawaz, M.; Ahmed, J.; Abbas, G. Energy-Efficient Battery Management System for Healthcare Devices. *J. Energy Storage* **2022**, *51*, 104358. [CrossRef]
11. Ghafari, A.; Mohammadi, E.; Dastjerdi, M.; Honarmand, S.; Radmoghadam, Z.A.; Akbari, S. Batteries Applications in the Biomedical Industry: A Review. *Nano Sci. Technol.* **2023**, *10*, 33–52. [CrossRef]
12. Tobola, A.; Korpok, O.; Leutheuser, H.; Schmitz, B.; Hofmann, C.; Struck, M.; Weigand, C.; Eskofier, B.; Heuberger, A.; Fischer, G. System Design Impacts on Battery Runtime of Wearable Medical Sensors. In Proceedings of the Mobile and Information Technologies in Medicine and Health, Prague, Czech Republic, 20–21 November 2014.
13. Chen, Y.; Jahier Pagliari, D.; Macii, E.; Poncino, M. Battery-Aware Design Exploration of Scheduling Policies for Multi-Sensor Devices. In *Proceedings of the 2018 Great Lakes Symposium on VLSI, Chicago, IL, USA, 23–25 May 2018*; Association for Computing Machinery: New York, NY, USA, 2018; pp. 201–206.
14. Shin, Y.; Choi, K.; Sakurai, T. Power Optimization of Real-Time Embedded Systems on Variable Speed Processors. In Proceedings of the 2000 IEEE/ACM International Conference on Computer-Aided Design, San Jose, CA, USA, 5–9 November 2000; pp. 365–368.
15. Dron, W.; Duquennoy, S.; Voigt, T.; Hachicha, K.; Garda, P. An Emulation-Based Method for Lifetime Estimation of Wireless Sensor Networks. In Proceedings of the 2014 IEEE International Conference on Distributed Computing in Sensor Systems, Marina Del Rey, CA, USA, 26–28 May 2014; pp. 241–248.
16. Fafoutis, X.; Elsts, A.; Vafeas, A.; Oikonomou, G.; Piechocki, R. On Predicting the Battery Lifetime of IoT Devices: Experiences from the SPHERE Deployments. In *Proceedings of the 7th International Workshop on Real-World Embedded Wireless Systems and Networks, Shenzhen, China, 4 November 2018*; Association for Computing Machinery: New York, NY, USA, 2018; pp. 7–12.
17. Gozuoglu, A. IoT-Enhanced Battery Management System for Real-Time SoC and SoH Monitoring Using STM32-Based Programmable Electronic Load. *Internet Things* **2025**, *30*, 101509. [CrossRef]
18. STMicroelectronics. *LPS27HHW: MEMS Pressure Sensor: 260-1260 hPa Absolute Digital Output Barometer with Water Resistant Package*; Datasheet LPS27HHW; STMicroelectronics: Geneva, Switzerland, 2019. Available online: https://www.st.com/resource/en/datasheet/lps27hhw.pdf (accessed on 23 October 2026).
19. STMicroelectronics. *STMicroelectronics Application Note AN4746: How to Optimize Power and Performance on STM32L4 and STM32L4+ MCUs*; Application Note AN4746; STMicroelectronics: Geneva, Switzerland, 2026. Available online: https://www.st.com/resource/en/application_note/an4746-how-to-optimize-power-and-performance-on-stm32l4-and-stm32l4-mcus-stmicroelectronics.pdf (accessed on 24 October 2026).
20. Maxim Integrated Products. *MAX17048/MAX17049 3µA 1-Cell/2-Cell Fuel Gauge with ModelGauge*; Datasheet MAX17048/MAX17049; Maxim Integrated: San Jose, CA, USA, 2016. Available online: https://www.analog.com/media/en/technical-documentation/data-sheets/max17048-max17049.pdf (accessed on 23 October 2026).
21. STMicroelectronics. *STM32CubeIDE*, version 2.1.1; STMicroelectronics: Geneva, Switzerland, 2026. Available online: https://www.st.com/en/development-tools/stm32cubeide.html (accessed on 24 October 2026).

22. STMicroelectronics. *STM32CubeMX*, version 6.17.0; STMicroelectronics: Geneva, Switzerland, 2026. Available online: https://www.st.com/en/development-tools/stm32cubemx.html (accessed on 24 October 2026).
23. STMicroelectronics. *STMicroelectronics Application Note AN4621: STM32L4 and STM32L4+ Ultra-Low-Power Features Overview*; Application Note AN4621; STMicroelectronics: Geneva, Switzerland, 2019. Available online: https://www.st.com/resource/en/application_note/an4621-stm32l4-and-stm32l4-ultralowpower-features-overview-stmicroelectronics.pdf (accessed on 10 October 2026).
24. STMicroelectronics. *Errata Sheet ES0318: STM32L431xx/432xx/433xx/442xx/443xx Device Errata, Errata Sheet ES0318*; STMicroelectronics: Geneva, Switzerland, 2024. Available online: https://www.st.com/resource/en/errata_sheet/es0318-stm32l433xx443xx-device-errata-stmicroelectronics.pdf (accessed on 21 October 2026).

Disclaimer/Publisher's Note: The statements, opinions and data contained in all publications are solely those of the individual author(s) and contributor(s) and not of MDPI and/or the editor(s). MDPI and/or the editor(s) disclaim responsibility for any injury to people or property resulting from any ideas, methods, instructions or products referred to in the content.